# Smart Regenerative Relays for Link-Adaptive Cooperative Communications

Tairan Wang, *Student Member, IEEE,* Georgios B. Giannakis, *Fellow, IEEE,* and Renqiu Wang, *Member, IEEE*

***Abstract*—Without being necessary to pack multiple antennas per terminal, cooperation among distributed single-antenna nodes offers resilience to shadowing and can, in principle, enhance the performance of wireless communication networks by exploiting the available space diversity. Enabling the latter however, calls for practically implementable protocols to cope with errors at relay nodes so that simple receiver processing can collect the diversity at the destination. To this end, we derive in this paper a class of strategies whereby decoded bits at relay nodes are scaled in power before being forwarded to the destination. The scale is adapted to the signal-to-noise-ratio (SNR) of the source-relay and the intended relay-destination links. With maximum ratio combining (MRC) at the destination, we prove that such link-adaptive regeneration (LAR) strategies effect the maximum possible diversity while requiring simple channel state information that can be pragmatically acquired at the relay. In addition, LAR exhibits robustness to quantization and feedback errors and leads to efficient use of power both at relay as well as destination nodes. Analysis and corroborating simulations demonstrate that LAR relays are attractive across the practical SNR range; they are universally applicable to multi-branch and multi-hop uncoded or coded settings regardless of the underlying constellation; and outperform existing alternatives in terms of error performance, complexity and bandwidth efficiency.**

***Index Terms*—Cooperative communications, adaptive transmissions, diversity order, relay strategies, regenerative relay, maximum-ratio-combining.**

## I. Introduction

At the cost of deploying multiple antennas collocated at the source ($S$) and destination ($D$) nodes of a wireless link, space-time communications have well-appreciated merits in terms of improving achievable rates and error performance through space diversity. Recently, interest has been growing towards migrating these benefits to cost-effective distributed scenarios where besides the direct link, information from $S$ to $D$ flows also through cooperating relay ($R$) nodes; see also Fig. 1. Even if $S, R, D$ nodes are equipped with a single-antenna, information replicas arriving at $D$ can be fused coherently using e.g., maximum ratio combining (MRC) to collect the available space diversity while also gaining resilience to shadowing effects [1]–[3].

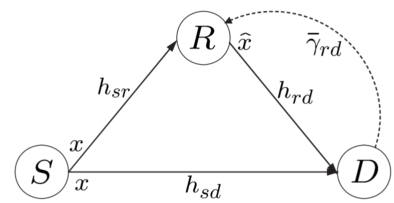

Fig. 1. The "molecule relay channel" model.

Critical to the performance of these cooperative communication networks are the combining mechanism at $D$ and the relay strategy at $R$. Both of these are challenged by possible errors at $R$ which constitute the main difference between collocated and distributed multi-antenna systems. Available relay protocols include:

- the non-regenerative *amplify-and-forward* (AF) strategy which achieves the available diversity with MRC, but may be less practical because it requires storage of analog waveforms at $R$ [4], [5];
- the regenerative *decode-and-forward* (DF) strategy which is simple and practical but loses the diversity benefits unless sophisticated combining is employed at $D$ to account for the reliability of the $S \to R \to D$ link [6]; and
- the *selective decode-and-forward* (SDF) strategy which relies on e.g., cyclic redundancy check (CRC) codes to detect errors at $R$ and selectively forward to $D$ only those correctly regenerated bits [7], [8]. SDF enables diversity at the expense of decoding delay and spectral efficiency loss incurred by the CRC codes.

Shannon's capacity of the simple $(S, R, D)$ triplet is unknown even in the absence of fading effects [9]. Nonetheless, information theoretic bounds have suggested the notion of (but not a practical implementation for) the so termed compress-and-forward (CF) relay strategy [10]. On the other hand, all implementable relay protocols are basically non-adaptive even though capacity-achieving point-to-point communication systems suggest transmissions which adapt to the intended links. Motivated by these considerations, the present paper develops a class of smart *link-adaptive regeneration* (LAR) strategies at the relay node(s) enabling the maximum possible diversity which can be guaranteed through the use of simple MRC at $D$. Without relying on CRC codes, LAR applies also to multi-

Paper approved by H. Minn, the Editor for Synchronization and Equalization of the IEEE Communications Society. Manuscript received December 17, 2006; revised May 10, 2007 and August 3, 2007. This work was supported through collaborative participation in the Communications and Networks Consortium sponsored by the U.S. Army Research Laboratory under the Collaborative Technology Alliance Program, Cooperative Agreement DAAD19-01-2-0011. The U.S. Government is authorized to reproduce and distribute reprints for Government purposes notwithstanding any copyright notation thereon. This paper was presented in part at the 40th Conference on Information Sciences and Systems, Princeton University, NJ, March 2006.

T. Wang and G. B. Giannakis are with the Department of Electrical and Computer Engineering, University of Minnesota, Minneapolis, MN 55455, USA (e-mail: {wang0822, georgios}@umn.edu).

R. Wang is with Qualcomm Incorporation, San Diego, CA 92121, USA (e-mail: rwang@qualcomm.com).

Digital Object Identifier 10.1109/TCOMM.2008.060688

branch and multi-hop uncoded or coded settings. Simulations corroborate the analytical results and demonstrate that LAR outperforms existing relay strategies in terms of average bit-error-probability (BEP) while exhibiting robustness to both quantization and feedback errors.

The rest of this paper is organized as follows. In Section II the problem statement is presented for the "molecule $(S, R, D)$ relay channel"; LAR strategies are introduced in Section III; and their performance is analyzed in Section IV. In Section V, results for the "molecule relay channel" are generalized and compared with various relaying strategies from several perspectives. Finally, simulations and conclusions are given in Sections VI and VII, respectively.

**Notation**: $(\cdot)^*$ denotes conjugation; $\mathcal{CN}(0,\sigma^2)$ the circular symmetric complex Gaussian distribution with zero mean and variance $\sigma^2$; $Re\{z\}$ the real part of a complex number $z$; $p(\gamma)$ denotes the probability density function of a random variable, and $\bar{\gamma} = E[\gamma]$ stands for its mean; and the $Q$-function is defined as $Q[x] := (1/\sqrt{2\pi})\int_x^\infty \exp(-t^2/2)dt$.

## II. Modeling and Problem Statement

Consider first the $S \to R \to D$ "molecule relay channel" depicted in Fig. 1. Suppose that symbols $x$ from $S$ and $\hat{x}$ from $R$ are transmitted over orthogonal channels; e.g., via time-division-multiplexing (TDM). With subscripts signifying the corresponding link, the pertinent input-output relationships are

$$y_{sr} = h_{sr}x + z_{sr}, y_{sd} = h_{sd}x + z_{sd}, y_{rd} = h_{rd}\sqrt{\alpha}\,\hat{x} + z_{rd} \quad (1)$$

where $y$ denotes received symbols, $z$ additive white Gaussian noise (AWGN) terms, $h$ the corresponding channel coefficients, and $\alpha$ represents a link-adaptive scalar which controls transmit power in the $R \to D$ link. We suppose operation under the following three conditions:

**c1.** *Wireless channels entail block Rayleigh fading propagation and AWGN at reception; i.e.,* $h_{sr} \sim \mathcal{CN}(0,\sigma_{sr}^2)$, $h_{sd} \sim \mathcal{CN}(0,\sigma_{sd}^2)$, $h_{rd} \sim \mathcal{CN}(0,\sigma_{rd}^2)$, *with* $\sigma_{sr}^2 := E\{|h_{sr}|^2\}$, $\sigma_{sd}^2 := E\{|h_{sd}|^2\}$, $\sigma_{rd}^2 := E\{|h_{rd}|^2\}$, *and* $z_{sr}, z_{sd}, z_{rd} \sim \mathcal{CN}(0, N_0)$. *Hence, the corresponding links exhibit instantaneous and average signal-to-noise-ratios (SNRs) given, respectively, by*

$$\gamma_{sr} := |h_{sr}|^2\bar{\gamma}, \gamma_{rd} := |h_{rd}|^2\bar{\gamma}, \gamma_{sd} := |h_{sd}|^2\bar{\gamma}, \bar{\gamma} := \mathcal{P}_x/N_0 \quad (2)$$

*and*

$$\bar{\gamma}_{sr} = \sigma_{sr}^2\bar{\gamma}, \quad \bar{\gamma}_{sd} = \sigma_{sd}^2\bar{\gamma}, \quad \bar{\gamma}_{rd} = \sigma_{rd}^2\bar{\gamma} \quad (3)$$

*where* $\mathcal{P}_x$ *denotes the average transmit-power of source symbols* $x$ *which are assumed drawn from a finite alphabet* $\mathcal{A}_x$ *with cardinality* $|\mathcal{A}_x|$.

Although Rayleigh fading is assumed in c1 for specificity, we can allow for any distribution encountered with practical fading channels including Ricean and Nakagami ones; we will test such channels with simulations. AWGN variances at $S$, $R$ and $D$ are assumed equal without loss of generality since all results in this paper depend on instantaneous or average SNRs and unequal noise variances can be absorbed in the corresponding $(\gamma_{sr}, \gamma_{rd}, \gamma_{sd})$ or $(\bar{\gamma}_{sr}, \bar{\gamma}_{rd}, \bar{\gamma}_{sd})$ triplets.

**c2.** *Symbols from* $S$ *are detected optimally (in the maximum-likelihood sense) at* $R$ *as*

$$\hat{x} = \arg\min_{x\in\mathcal{A}_x} |y_{sr} - h_{sr}x|^2 \quad (4)$$

*and forwarded to* $D$ *with power scaling adapted to: either the instantaneous* $\gamma_{sr}$ *and* $\gamma_{rd}$, *as*

$$\alpha_{inst} := \frac{\min(\gamma_{sr},\gamma_{rd})}{\gamma_{rd}} = \begin{cases} \gamma_{sr}/\gamma_{rd}, & \text{if } \gamma_{sr} < \gamma_{rd} \\ 1, & \text{if } \gamma_{sr} \geq \gamma_{rd} \end{cases} \quad (5)$$

*or, the instantaneous* $\gamma_{sr}$ *and the average* $\bar{\gamma}_{rd}$, as

$$\alpha := \frac{\min(\gamma_{sr},\bar{\gamma}_{rd})}{\bar{\gamma}_{rd}} = \begin{cases} \gamma_{sr}/\bar{\gamma}_{rd}, & \text{if } \gamma_{sr} < \bar{\gamma}_{rd} \\ 1, & \text{if } \gamma_{sr} \geq \bar{\gamma}_{rd}. \end{cases} \quad (6)$$

Fading coefficients of all links are supposed known at receiving ends via training (pilot) symbols sent from the transmitting ends. For instance, the instantaneous $\gamma_{sr}$ used in (5) and (6) can be pragmatically acquired at $R$ using a sufficient number of training symbols with arbitrarily high accuracy. However, knowing the instantaneous $\gamma_{rd}$ at $R$ is not as immediate because it must be estimated at $D$ and fed back to $R$. Depending on how fast the link varies, the overhead due to frequent feedback may be prohibitive and the feedback may be outdated. For these reasons, scaling with $\alpha_{inst}$ as in (5) becomes more challenging if the $R \to D$ link varies fast.

Nonetheless, LAR based on $\alpha_{inst}$ (henceforth abbreviated as LAR-$\alpha_{inst}$) will benchmark the error performance of LAR based on the power scaling $\alpha$ in (6). This second LAR-$\alpha$ scheme is clearly practical even for relatively fast fading channels since $\bar{\gamma}_{rd}$ can be easily estimated so long as the channel remains stationary. Note also that the overhead for feeding back the statistical channel state information (CSI) $\bar{\gamma}_{rd}$ is certainly affordable. Besides $\alpha_{inst}$ and $\alpha$, we will consider also quantized and generalized alternatives which even account for estimation and feedback errors in $\bar{\gamma}_{rd}$.

Having described processing options at $R$, let us consider demodulation at $D$.

**c3.** *Using weights* $w_{sd} = h_{sd}^*$ *and* $w_{rd} = h_{rd}^*\sqrt{\alpha}$, *MRC is performed at* $D$ *to obtain*

$$\hat{x}_d^{MRC} = \arg\min_{x\in\mathcal{A}_x} |w_{sd}y_{sd} + w_{rd}y_{rd} - (w_{sd}h_{sd} + w_{rd}h_{rd}\sqrt{\alpha})x|^2. \quad (7)$$

In order to obtain $\hat{x}_d^{MRC}$ from (7), $D$ needs to have available only $h_{sd}$ of the direct $S \to D$ link and the product $h_{rd}\sqrt{\alpha}$ of the $R \to D$ link, both of which are computable via training.

Notice also that unlike existing relay strategies where transmit-power at $R$ is scaled by a constant not dependent on the channel (e.g., $\alpha = 1$ for DF), the *soft power scaling* with $\alpha \in [0, 1]$ is adapted to link-SNR values that can be pragmatically obtained. In accordance with (6), $\alpha$ relays information to $D$ at full power when the $S \to R$ link is more reliable than the $R \to D$ link; otherwise, $\alpha$ scales power down (even to zero) in order to mitigate errors at the $S \to R \to D$ branch of the MRC. It will turn out that this simple but basic operation renders relay channels diversity achieving without CRC decoding at $R$ which is used in e.g., SDF at the price of delay, complexity and bandwidth efficiency loss.

Under c1-c3, our objective in this paper is to prove that LAR-$\alpha$ enables the maximum possible diversity for any constellation not only in the molecule relay channel of Fig. 1, but also in multi-branch and multi-hop settings. We further wish to show that proper modifications of $\alpha$ can accommodate reduced-overhead feedback as well as quantization and feedback errors in $\bar{\gamma}_{rd}$. Our final goal will be to compare LAR-$\alpha$ strategies with existing relay protocols in terms of average BEP and power required at the relay.

## III. LAR STRATEGIES

Besides $\alpha_{inst}$ in (5) and $\alpha$ in (6), there are alternative soft relay options accounting for various practical issues. In this sense, LAR that we develop in this section refers to a class of strategies.

### A. Soft Power Scaling with Errors

For $R$ to scale power using $\alpha$ in (6), it is necessary for $D$ to feed back the real number $\bar{\gamma}_{rd}$. To enhance the potential of this operation for practical deployment we consider here that $D$ feeds back an imperfect version of $\bar{\gamma}_{rd}$. Since imperfections may depend on the specific $\bar{\gamma}_{rd}$ value, we consider a worst-case scenario where errors arising due to e.g., quantization and/or feedback, take the maximum possible value. Clearly, BEP performance in this scenario will upper bound the actual BEP. With this maximum error, suppose that instead of $\bar{\gamma}_{rd}$, $R$ receives $\beta\bar{\gamma}_{rd}$, for some $\beta > 0$. For example, to describe a worst-case $\beta\bar{\gamma}_{rd}$ that allows for imperfect feedback 3dB higher than the true $\bar{\gamma}_{rd}$, we set $\beta = 2$. For a general $\beta$, $\alpha$ in (6) is expressed as

$$\alpha(\beta) := \frac{\min(\gamma_{sr}, \beta\bar{\gamma}_{rd})}{\beta\bar{\gamma}_{rd}} = \begin{cases} \gamma_{sr}/(\beta\bar{\gamma}_{rd}), & \text{if } \gamma_{sr} < \beta\bar{\gamma}_{rd} \\ 1, & \text{if } \gamma_{sr} \geq \beta\bar{\gamma}_{rd} \end{cases} \quad (8)$$

which clearly subsumes (6) when $\beta = 1$. Note that adapting power using $\alpha(\beta)$ in (8) may rely on a quantized $\bar{\gamma}_{rd}$ even if the soft scaling $\alpha(\beta)$ has analog amplitude.

### B. Hard Power Scaling

For a given number of bits $N_q$, we can also scale power at the relay using a quantized version of $\alpha(\beta)$ itself. Specifically, with $M = 2^{N_q}$ denoting the number of quantization intervals, we can adjust power using a (hard) scaling coefficient

$$\alpha_q(N_q, \beta) := \frac{\text{round}[\alpha(\beta)(M-1)]}{M-1} \quad (9)$$

where $\text{round}[x]$ denotes the rounding operation to the nearest integer.

For one-bit quantization ($N_q = 1$) and $\beta = 2$, the quantized scaling coefficient in (9) reduces to a simple on-off relaying strategy for which

$$\alpha_{on-off} := \alpha_q(1,2) = \begin{cases} 0, & \text{if } \gamma_{sr} < \bar{\gamma}_{rd}, \\ 1, & \text{if } \gamma_{sr} \geq \bar{\gamma}_{rd}. \end{cases} \quad (10)$$

### C. Average Power Scaling

Instead of $\alpha(\beta)$ or quantized versions of it, it is also possible to average $\alpha_{inst}$ with respect to $\gamma_{rd}$; e.g., to scale power at $R$ using

$$\begin{aligned} \alpha' &:= E_{\gamma_{rd}}\left[\frac{\min(\gamma_{sr}, \gamma_{rd})}{\gamma_{rd}}\right] \\ &= \int_0^{\gamma_{sr}} \frac{1}{\bar{\gamma}_{rd}} \exp(-\frac{\gamma_{rd}}{\bar{\gamma}_{rd}}) d\gamma_{rd} + \int_{\gamma_{sr}}^{\infty} \frac{1}{\bar{\gamma}_{rd}} \frac{\gamma_{sr}}{\gamma_{rd}} \exp(-\frac{\gamma_{rd}}{\bar{\gamma}_{rd}}) d\gamma_{rd} \\ &= 1 - \exp(\frac{\gamma_{sr}}{\bar{\gamma}_{rd}}) + \frac{\gamma_{sr}}{\bar{\gamma}_{rd}} \mathrm{E}_1(\frac{\gamma_{sr}}{\bar{\gamma}_{rd}}) \end{aligned} \quad (11)$$

where for the second equality we used that $\gamma_{rd}$ is Rayleigh distributed and $\mathrm{E}_1(x)$ is the $\mathrm{E}_n$-function with $n = 1$ [11].

When only average $\bar{\gamma}_{sr}$ and $\bar{\gamma}_{rd}$ are available at $R$, as in e.g., non-coherent operation, it is possible to use

$$\bar{\alpha} := \frac{\min(\bar{\gamma}_{sr}, \bar{\gamma}_{rd})}{\bar{\gamma}_{rd}} = \begin{cases} \bar{\gamma}_{sr}/\bar{\gamma}_{rd}, & \text{if } \bar{\gamma}_{sr} < \bar{\gamma}_{rd} \\ 1, & \text{if } \bar{\gamma}_{sr} \geq \bar{\gamma}_{rd}. \end{cases} \quad (12)$$

**Remark 1:** A power scaling coefficient was advocated in [12] by approximately maximizing the output SINR at $D$, without any diversity analysis. This scaling is denoted here as (corresponds to $\alpha_{r_1}^{(2)}$ in [12])

$$\alpha'' := \frac{(1 - 2P_{sr}^b)}{1 + 4P_{sr}^b(1 - P_{sr}^b)\bar{\gamma}_{rd}} \quad (13)$$

where $P_{sr}^b = Q[\sqrt{2\gamma_{sr}}]$ is the instantaneous error probability at $R$.

Summarizing, "soft" and "hard" power scaling of relay transmissions can be effected through any of the coefficients in (5), (6) or (8) to (12). The difficulty in acquiring these coefficients varies depending on operational conditions. But their common characteristic is that each captures through a different performance metric the quality of $S \to R$ and $R \to D$ links. In fact, the various LAR options can be viewed as implementing DF relaying with channel-adaptive power allocation – a subject also considered earlier in [12], [13] and [14]. However, these approaches either need to forward or feed back *instantaneous* CSI, or cannot provably ensure full diversity at $D$. The next section shows that LAR-$\alpha$ can achieve full diversity with pragmatically affordable CSI feedback.

## IV. PERFORMANCE ANALYSIS OF LAR

Starting with $\alpha(\beta)$ in (8), we will analyze in this section the performance of LAR-$\alpha(\beta)$ strategies using as metrics the diversity exponents of the average and outage error probability.

### A. Diversity Analysis for $\alpha(\beta)$

Diversity gain (a.k.a. diversity order) $G_d$ is defined as the negative exponent in the average BEP when $\bar{\gamma} \to \infty$, i.e., $G_d := \lim_{\bar{\gamma}\to\infty} -\frac{\log E[P^b]}{\log \bar{\gamma}}$, which for sufficiently high SNR implies

$$E[P^b] \overset{\bar{\gamma}\to\infty}{\approx} (G_c\bar{\gamma})^{-G_d} \quad (14)$$

where $G_c$ denotes the coding gain. For symbol-by-symbol demodulation of uncoded transmissions, $G_c$ depends solely on the constellation and the transmit power. On the other hand, $G_d$ affects more critically the average BEP at high SNR. The maximum possible value of $G_d$ that can be achieved for a given channel is referred to as full diversity.

For clarity in exposition, we will first analyze the diversity of LAR-$\alpha(\beta)$ for BPSK. Generalization to higher constellations will be discussed afterwards. With BPSK, $x$ transmitted from $S$ can only take one of the two values: $x = \sqrt{\mathcal{P}_x}$, or, $x = -\sqrt{\mathcal{P}_x}$. Correspondingly, the detected $\hat{x}$ at the relay can only be $\hat{x} = x$, or, $\hat{x} = -x$. For each case, the output at $D$ is:

$$y_D = w_{rd}y_{rd} + w_{sd}y_{sd} = \begin{cases}(w_{sd}h_{sd}+w_{rd}h_{rd}\sqrt{\alpha(\beta)})x+w_{rd}z_{rd}+w_{sd}z_{sd}, \text{if } \hat{x}=x \\ (w_{sd}h_{sd}-w_{rd}h_{rd}\sqrt{\alpha(\beta)})x+w_{rd}z_{rd}+w_{sd}z_{sd}, \text{if } \hat{x}=-x.\end{cases} \quad (15)$$

Since BPSK symbols are real-valued, it suffices to consider only the real part $y = Re\{y_D\}$, which is a real Gaussian random variable with zero mean and variance $\sigma^2 := (|w_{rd}|^2 + |w_{sd}|^2)N_0/2$. The instantaneous BEP at $D$ can thus be expressed as

$$\begin{aligned} P^b = &[1 - P^b_{sr}(\gamma_{sr})]\int_0^\infty \frac{1}{\sqrt{2\pi\sigma^2}} \\ &\times \exp\left\{-\frac{[y+(w_{sd}h_{sd}+w_{rd}h_{rd}\sqrt{\alpha(\beta)})x]^2}{2\sigma^2}\right\}dy \\ &+P^b_{sr}(\gamma_{sr})\int_0^\infty \frac{1}{\sqrt{2\pi\sigma^2}} \\ &\times \exp\left\{-\frac{[y+(w_{sd}h_{sd}-w_{rd}h_{rd}\sqrt{\alpha(\beta)})x]^2}{2\sigma^2}\right\}dy. \end{aligned} \quad (16)$$

With the substitutions $w_{sd} = h^*_{sd}$ and $w_{rd} = h^*_{rd}\sqrt{\alpha(\beta)}$, (16) can be re-written compactly in terms of the $Q$-function as

$$\begin{aligned} P^b = &\left\{1-Q\left[\sqrt{2\gamma_{sr}}\right]\right\}Q\left[\sqrt{2(\gamma_{sd}+\gamma'_{rd})}\right] \\ &+Q\left[\sqrt{2\gamma_{sr}}\right]Q\left[\frac{\sqrt{2}(\gamma_{sd}-\gamma'_{rd})}{\sqrt{\gamma_{sd}+\gamma'_{rd}}}\right] \end{aligned} \quad (17)$$

where $\gamma'_{rd} := \alpha(\beta)|h_{rd}|^2\mathcal{P}_x/N_0 = \alpha(\beta)\gamma_{rd}$. Taking expectation over the instantaneous SNRs, (17) yields the average BEP $E[P^b]$. Note that the steps leading to (16) apply universally to all the power scaling coefficients we presented in Section III.

To proceed, we upper bound $E[P^b]$ as $E[P^b] \le E[P^b_1] + E[P^b_2]$, where

$$P^b_1 := Q\left[\sqrt{2(\gamma_{sd}+\gamma'_{rd})}\right] \quad (18)$$

$$P^b_2 := Q\left[\sqrt{2\gamma_{sr}}\right]Q\left[\frac{\sqrt{2}(\gamma_{sd}-\gamma'_{rd})}{\sqrt{\gamma_{sd}+\gamma'_{rd}}}\right]. \quad (19)$$

We contend that both $E[P^b_1]$ and $E[P^b_2]$ decay with the same exponent (diversity order), two. First, we establish this result for $E[P^b_1]$.

**Lemma 1:** *Under c1-c3, the expectation $E[P^b_1]$ can be upper bounded by a term $\tilde{P}^b_1$, which decays with exponent equal to two; i.e., $E[P^b_1] \le \tilde{P}^b_1$ and*

$$\lim_{\bar{\gamma}\to\infty} -\frac{\log \tilde{P}^b_1}{\log \bar{\gamma}} = 2. \quad (20)$$

*Proof:* See Appendix A.

To appreciate (20), recall that $E[P^b]$ achieves full diversity whenever the relay is forwarding the correct symbol ($\hat{x} = x$), which corresponds either to a system with a single transmit-antenna and two co-located receive-antennas, or, to a system with two co-located transmit-antennas and a single receive-antenna.

Turning back our attention to (19), the next proposition upper bounds $E[P^b_2]$.

**Lemma 2:** *Under c1-c3, the expectation $E[P^b_2]$ can be upper bounded by a term $\tilde{P}^b_2$, which decays with exponent equal to two; i.e., $E[P^b_2] \le \tilde{P}^b_2$ and*

$$\lim_{\bar{\gamma}\to\infty} -\frac{\log \tilde{P}^b_2}{\log \bar{\gamma}} = 2. \quad (21)$$

*Proof:* See Appendix B.

One can gain additional insight about Lemma 2 by inspecting (19), where $\gamma'_{rd} := \alpha(\beta)\gamma_{rd}$ is a monotonically increasing function of $\gamma_{sr}$ [cf. (8)]. As $\gamma_{sr}$ in (19) increases, the second Q-factor increases while the first Q-factor decreases. Optimizing this tradeoff guides the adaptation of $\alpha(\beta)$ depending on the quality of the $S \to R$ and $R \to D$ links.

When BPSK is employed, (20) and (21) establish that LAR-$\alpha(\beta)$ achieves full diversity. Interestingly, even when $D$ feeds back a quantized version of $\bar{\gamma}_{rd}$ to $R$, our upper bound analysis implies that full diversity can still be guaranteed for any soft $\alpha(\beta)$. However, the value of $\beta$ does affect the coding gain, as we will demonstrate in the simulations.

For higher-order constellations, we consider the symbol-error-probability (SEP) of LAR-$\alpha(\beta)$. With $P^s_{sr}(\gamma_{sr})$ denoting the SEP from $S$ to $R$, the MRC branches at $D$ receive identical symbols from $S$ and $R$ with probability $1-P^s_{sr}(\gamma_{sr})$; and non-identical ones with probability $P^s_{sr}(\gamma_{sr})$. Hence, (16) carries over to higher-order constellations. The difference is that $Q[\sqrt{2\gamma}]$ factors in (17) must be replaced by $Q[\sqrt{k\gamma}]$, where $k$ is a constellation-specific constant ($k = 2$ for BPSK). But since diversity pertains to high SNR behavior, it is not affected by such constants (also true with co-located antenna systems). Hence, Lemma 1 still holds true for general constellations. To ensure full diversity, we need to show that Lemma 2 is also valid for general constellations; i.e., that when there is a detection error at $R$, the SEP $P^s_e$ at $D$ decays with full diversity slope $-G_d$. Happening with probability $P^s_{sr}(\gamma_{sr})$, $P^s_e$ can be bounded by the worst case when the decoded symbol at $R$ is the farthest point in the constellation from the actual symbol sent from $S$. In such a case, the final expression of the SEP will have form identical to that for BPSK within a scale depending on $d_{\min}$ and $d_{\max}$, which denote the minimum and maximum Euclidean distances between points in the constellation, respectively.[1] Thus, Lemma 2 is still valid, which establishes that:

**Proposition 1:** *Under c1-c3, soft power scaling with $\alpha(\beta)$ in* (8) *achieves full diversity regardless of the underlying constellation.*

[1]For a detailed derivation of related claims in a different context see [6, Subsection II-F].

Since Proposition 1 holds for any $\beta > 0$ in (8), an interesting result is that without any feedback from $D$, full diversity can still be achieved with a simple choice of $\alpha(\beta) = \min(\gamma_{sr}, \bar{\gamma}_{sr})/\bar{\gamma}_{sr}$ at $R$. In practice, however, $R$ needs $\bar{\gamma}_{rd}$ to modify its transmit power appropriately for a low SEP at $D$.

Next, we analyze the diversity when hard power scaling is employed at $R$.

### B. Diversity Analysis for $\alpha_q$

Here we consider the quantized power scaling at $R$ with $N_q$ bits and any $\beta > 0$ as in (9). The next proposition establishes a negative result with regards to diversity.

**Proposition 2:** *Under c1-c3, hard power scaling with $\alpha_q(N_q, \beta)$ in (9) cannot guarantee full diversity gain 2. In fact, the diversity order with $N_q = 1$ is just 1. The latter holds true also for the $\alpha_{on-off}$ scaling in (10).*
*Proof:* See Appendix C.

Proposition 2 establishes that diversity may be lost for sufficiently high SNR when using a quantized power scaling coefficient – a fact that we will also confirm with simulations. Somewhat surprisingly though, simulations will illustrate that full diversity is attained with $N_q > 1$ over practical SNR values.

**Remark 2:** Since the averages $\bar{\gamma}_{sr}$ and $\bar{\gamma}_{rd}$ are constant, the power scaling $\bar{\alpha}$ in (12) is non-adaptive. As a result, $\bar{\alpha}$ leads to diversity loss for the same reason that DF does too.

**Remark 3:** Equations (11) and (13) offer two additional power scalings. Diversity analysis for LAR$-\alpha'$ and LAR$-\alpha''$ is complicated and goes beyond the scope of this paper. Compared to these two choices, $\alpha$ in (6) is simpler and also leads to closed-form diversity analysis. Nevertheless, $\alpha'$ and $\alpha''$ will be considered in the simulated comparisons of Section VI.

### C. Outage Analysis

Besides average BEP, it is also possible to define the diversity gain based on the outage probability $P_{out}$ after replacing the left hand side of (14) with

$$P_{out} := \Pr(P^b(\boldsymbol{\gamma}) > P_0) = \int_{P^b(\boldsymbol{\gamma}) > P_0} p(\boldsymbol{\gamma}) d\boldsymbol{\gamma} \qquad (22)$$

where $P_0$ is a maximum acceptable error probability and $P^b(\boldsymbol{\gamma})$ denotes the BEP conditioned on the instantaneous SNR vector $\boldsymbol{\gamma} := [\gamma_{sr}, \gamma_{rd}, \gamma_{sd}]$. Using (22), it follows readily that

$$\begin{aligned} E[P^b] &= \int_{P^b(\boldsymbol{\gamma}) > P_0} P^b(\boldsymbol{\gamma}) p(\boldsymbol{\gamma}) d\boldsymbol{\gamma} + \int_{P^b(\boldsymbol{\gamma}) \le P_0} P^b(\boldsymbol{\gamma}) p(\boldsymbol{\gamma}) d\boldsymbol{\gamma} \\ &\geq \int_{P^b(\boldsymbol{\gamma}) > P_0} P_0 p(\boldsymbol{\gamma}) d\boldsymbol{\gamma} = P_0 P_{out}. \end{aligned} \qquad (23)$$

The implication of (23) is that whichever strategy achieves full diversity for $E[P^b]$, it also achieves full diversity for $P_{out}$. The converse is not true in general. Hence, the diversity claim for $\alpha(\beta)$ in Proposition 1 still holds true for $P_{out}$.

As an example of a strategy achieving full diversity for $P_{out}$ but not for $E[P^b]$, consider the on-off power scaling. In Proposition 2, we proved that full diversity cannot be achieved with the $\alpha_{on-off}$ coefficient in (10), where the threshold is only a function of $\gamma_{sr}$ and $\bar{\gamma}_{rd}$ but not a function of the target BEP $P_0$ in (22). In fact, when $P_0$ is available at $R$, one can design an on-off strategy according to $P_0$ to effect a full diversity exponent in $P_{out}$. For example, the counterpart of an on-off strategy in SDF has been proposed in [3], where full diversity is achieved for rate outage probability, which is defined as the probability that the maximum average mutual information falls below a target rate.

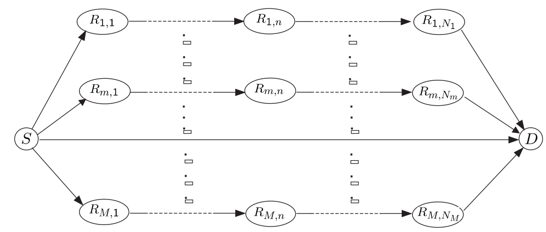


Fig. 2. A multi-hop multi-branch system.

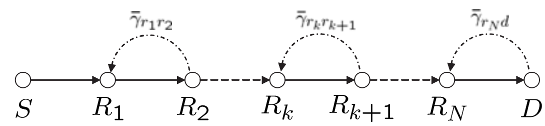


Fig. 3. LAR-$\alpha$ in one branch with multi-hop cooperation.

## V. Generalizations and Comparisons

Here we generalize the results of Section IV for the molecule relay channel to multi-branch, multi-hop, uncoded and coded settings. We further compare LAR-$\alpha$ with existing popular relay strategies including AF, DF and SDF.

### A. General Cooperative Systems

Consider a cooperative system with $M+1$ branches, $B_0, B_1, \ldots, B_M$, as depicted in Fig. 2. Without loss of generality, let $B_0$ denote the direct link. Branch $B_m$ consists of $N_m$ relays and $R_{m,n}$ denotes the $n^{th}$ node in branch $B_m$, $n = 1, \ldots, N_m$ and $m = 1, \ldots, M$. As usual, access across branches is assumed orthogonal (e.g., via TDMA or FDMA) and the relays do not perform MRC. Under these conditions, it suffices to focus on one branch only.

As shown in Fig. 3, $R_k$ only needs feedback of $\bar{\gamma}_{r_kr_{k+1}}$ from $R_{k+1}$, and feeds back $\bar{\gamma}_{r_{k-1}r_k}$ to $R_{k-1}$, $k = 1, \ldots, N$. The scaling coefficients $\alpha$ per branch are [cf. (6)]

$$\begin{cases} \alpha_{r_1} := \frac{\min(\gamma_{sr_1}, \bar{\gamma}_{r_1r_2})}{\bar{\gamma}_{r_1r_2}} \\ \alpha_{r_k} := \frac{\min(\alpha_{r_{k-1}}\gamma_{r_{k-1}r_k}, \bar{\gamma}_{r_kr_{k+1}})}{\bar{\gamma}_{r_kr_{k+1}}} \\ \alpha_{r_N} := \frac{\min(\alpha_{r_{N-1}}\gamma_{r_{N-1}r_N}, \bar{\gamma}_{r_Nd})}{\bar{\gamma}_{r_Nd}} \end{cases} \qquad (24)$$

where $k = 2, \ldots, N-1$. Notice that the product $\alpha_{r_{k-1}}\gamma_{r_{k-1}r_k}$ can be acquired at $R_k$ via training, and the exact value of $\gamma_{r_{k-1}r_k}$ is not needed at $R_k$. In other words, each relay scales its transmit power even during the training phase. As we mentioned earlier, the requirement of $R_k$ to feed back

TABLE I
COMPARISON OF VARIOUS RELAYING STRATEGIES.

| | Required CSI | Diversity Gain | Practical Considerations |
|---|---|---|---|
| AF | non-local CSI | full | analog signal storage |
| DF | local CSI | not full | practical |
| SDF | local CSI, CRC | full (perfect CRC) | bandwidth loss |
| LAR-$\alpha$ | local CSI, $\bar{\gamma}_{rd}$ at $R$ | full | accuracy of $\bar{\gamma}_{rd}$ |

the average SNR to $R_{k-1}$ is easy to meet in practice. Then Proposition 1 can be generalized to this scenario.

Turning our attention to coded systems, recall that each relay in LAR always takes a hard symbol decision before soft power scaling and forwarding. Thus, if we allow $R$ to re-encode the decoded bits and forward the parity check bits instead of the information bits, we can readily wed the coded cooperation schemes of [7] with any LAR strategy. Finally, Proposition 1 holds true wherever $R$ is close to $S$, close to $D$, or anywhere in between. For this reason, the merits of LAR-$\alpha$ apply regardless of the relative SNR as we will also confirm with simulations.

In the next two subsections, we compare different relay strategies from several perspectives. Table I summarizes these comparisons for the molecule relay channel.

### B. Power Efficiency

In addition to the diversity exponent $G_d$, the average BEP in (14) is critically affected (especially over the low to medium SNR range) by the coding gain $G_c$. For a given transmit-power $\mathcal{P}_x$ and any average SNR triplet ($\bar{\gamma}_{sr}$, $\bar{\gamma}_{rd}$, $\bar{\gamma}_{sd}$), the coding gain in turn depends primarily on how efficiently power is utilized at the relay. Hence, it is important to assess the average power $\bar{\mathcal{P}}_R$ at $R$ for the existing (AF, DF, SDF) and the proposed LAR strategies.

In both DF and AF, $R$ transmits with fixed average power $\mathcal{P}_x$. While in SDF, $R$ transmits with power $\mathcal{P}_x$ if and only if CRC detects no errors. Since the ability of a given CRC code to detect errors depends on the size of the frame, $\bar{\mathcal{P}}_R$ in SDF clearly depends on the frame length.

In LAR, the average transmit power depends on the scaling coefficient. When $\gamma_{rd}$ is available at $R$, LAR-$\alpha_{inst}$ can be implemented and the average transmit power at $R$ is [cf. (5)]

$$E[\alpha_{inst}\mathcal{P}_x]=\mathcal{P}_x E\left[\frac{\min(\gamma_{sr},\gamma_{rd})}{\gamma_{rd}}\right]=\mathcal{P}_x\frac{\bar{\gamma}_{sr}}{\bar{\gamma}_{rd}}\log\left[1+\frac{\bar{\gamma}_{rd}}{\bar{\gamma}_{sr}}\right] \quad (25)$$

where for the last equality we used the Rayleigh distribution for the channel [15, pp. 44-46]. When LAR relies on $\alpha$ [cf. (6)] or $\alpha_{on-off}$ [cf. (10)], we have respectively

$$E[\alpha\mathcal{P}_x]=\mathcal{P}_x E\left[\frac{\min(\bar{\gamma}_{sr},\bar{\gamma}_{rd})}{\bar{\gamma}_{rd}}\right]=\mathcal{P}_x\frac{\bar{\gamma}_{sr}}{\bar{\gamma}_{rd}}\left[1-\exp\left(-\frac{\bar{\gamma}_{rd}}{\bar{\gamma}_{sr}}\right)\right] \quad (26)$$

$$E[\alpha_{on-off}\mathcal{P}_x]=\mathcal{P}_x\exp\left(-\frac{\bar{\gamma}_{rd}}{\bar{\gamma}_{sr}}\right). \quad (27)$$

Likewise, for $\alpha'$ we find [cf. (11) and (5)]

$$\bar{\mathcal{P}}_R=E[\alpha'\mathcal{P}_x]=E[\alpha_{inst}\mathcal{P}_x]=\mathcal{P}_x\frac{\bar{\gamma}_{sr}}{\bar{\gamma}_{rd}}\log\left[1+\frac{\bar{\gamma}_{rd}}{\bar{\gamma}_{sr}}\right]. \quad (28)$$

Finally, since for $\alpha''$ we have no closed-form for $E[\alpha''\mathcal{P}_x]$, we will calculate its value numerically.

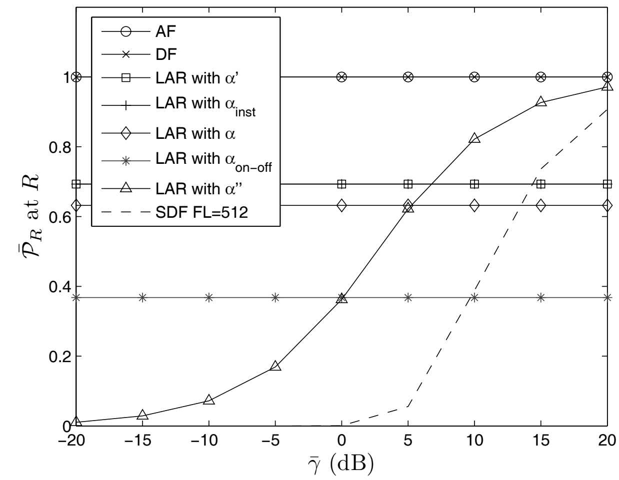


Fig. 4. Average transmit power at the relay for various relay strategies.

**Example:** For a graphical comparison, we substitute $\mathcal{P}_x = 1$, $\bar{\gamma} = \bar{\gamma}_{sr} = \bar{\gamma}_{rd}$ in (25)-(28) and depict $\bar{\mathcal{P}}_R$ versus $\bar{\gamma}$ in Fig. 4 for the various relay strategies. Notice that DF and AF consume the highest power $\bar{\mathcal{P}}_R = 1$ at the relay. Relative to them, LAR with $\alpha_{inst}$ $(\alpha)$ saves more than 30% (35%) in power. LAR-$\alpha_{on-off}$ is most power efficient but as we saw in Proposition 2 it leads to diversity loss. Relay power with SDF and LAR-$\alpha''$ is SNR dependent. (Both curves are obtained numerically with the frame length (FL) for SDF set to FL=512).

Besides power efficiency at the relay, it is important to assess how efficiently power is utilized at the destination. To highlight the merits of LAR-$\alpha$ in this respect, consider the extreme case where the $R \to D$ link is perfect, i.e., $\bar{\gamma}_{rd} \to \infty$, which reduces the molecule relay setup to the non-cooperative system with a single transmit-antenna and two co-located receive-antennas. In this system, $R$ does not have to transmit at all. Differently said, if $R$ transmits then power is wasted. Here DF, AF and SDF are not good choices because they waste too much power to transmit over a perfect channel, while LAR-$\alpha$ saves power since $\alpha \to 0$.

### C. Practical Considerations

Without any CSI of the $R \to D$ link available at the relay, DF with MRC at the destination is the simplest and most practical approach when the $S \to R$ link is reliable. However, simple MRC at the destination can not guarantee full diversity [16]. To achieve full diversity with DF, the destination needs instantaneous CSI of the $S \to R$ link along with proper combining [6].

Full diversity can be achieved with AF if MRC is performed at $D$. The latter combines the direct copy $y_{sd} = h_{sd}x + z_{sd}$ with the relay copy given by $y_{rd} = h_{rd}A(h_{sr}x+z_{sr})+z_{rd} = Ah_{sr}h_{rd}x+z_{rd}^{AF}$, where $z_{rd}^{AF} := Ah_{rd}z_{sr}+z_{rd}$ and $A$ denotes the amplification factor in AF. Because $z_{sd}$ and $z_{rd}^{AF}$ have unequal powers, $D$ must know $h_{rd}$ to equalize them prior to MRC. In addition, $D$ must know the product $h_{sr}h_{rd}$ to perform MRC. But requiring knowledge of $h_{rd}$ and $h_{sr}h_{rd}$ is

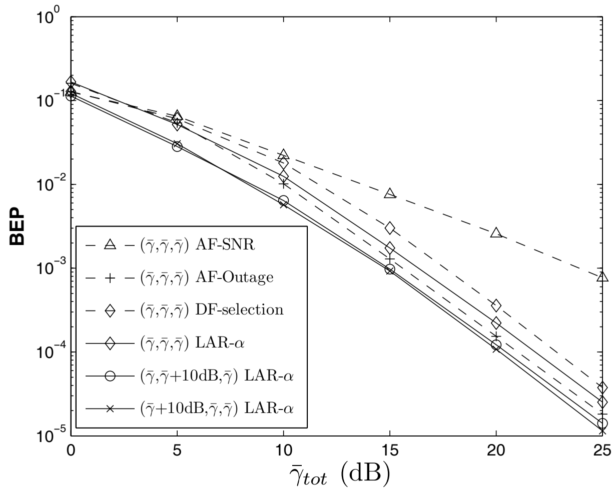


Fig. 5. BEP comparison for LAR-$\alpha$ with various channel SNR settings.

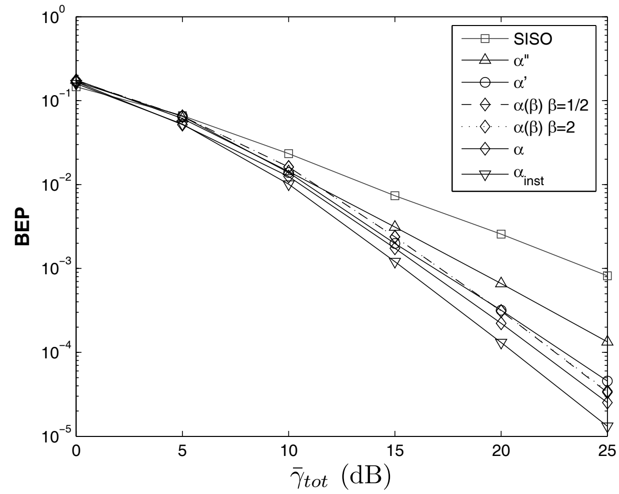


Fig. 6. BEP comparison of various LAR scaling factors.

tantamount to requiring $h_{sr}$ and $h_{rd}$. Hence, similar to DF, the AF strategy too relies on $D$ having knowledge of the instantaneous CSI of the $S \rightarrow R$ link; otherwise full diversity cannot be assured [4] [5].

With additional CRC bits, SDF offers an attractive strategy allowing the destination to perform only simple MRC at the expense of spectral-efficiency loss. To reduce this loss, the CRC frame should be relatively large. But increasing the frame length in turn decreases the probability of decoding the source message correctly at the relay, and thus downgrades the role of the relay in aiding the decoding process at the destination. This tradeoff restrains the error performance of SDF, rendering it more suitable when the $S \rightarrow R$ link has medium or high SNR quality.

In this paper, we advocated a novel LAR-$\alpha$ strategy enabling the relay to be smart and adaptive by softly adjusting its transmit-power. Exploiting average CSI of the $R \rightarrow D$ link, the relay adjusts its transmit-power so that the destination only needs to perform simple MRC. Sending back the average $\bar{\gamma}_{rd}$ is certainly realistic and can be implemented through a low-rate feedback channel. Even when the latter introduces errors, we have shown that LAR-$\alpha$ can achieve full diversity. Furthermore, LAR-$\alpha$ exhibits robustness to quantization errors and has been generalized to various scenarios as outlined in Subsection V-A.

As a byproduct, our results in this paper also demonstrate that *the diversity gain depends on how much knowledge is available at the relays or the destination, but not on whether the relay is regenerative or not.*

## VI. Simulations

Here we rely on simulations to test various scenarios and relay options for practical SNR values. Unless otherwise specified, QPSK is used throughout with average bit SNR $\bar{\gamma} = \mathcal{P}_x/(2N_0)$. Because different strategies require different transmit power at the relay, we use as figure of merit the aggregate average SNR $\bar{\gamma}_{tot}$ at the source and relays.

**Test Case 1 (different SNR setups):** In Fig. 5, we consider representative magnitudes of fading setups corresponding to those in which $R$ is located either close to the source, close to the destination, or equi-distant from both; the corresponding average SNRs triplets $(\bar{\gamma}_{sr}, \bar{\gamma}_{rd}, \bar{\gamma}_{sd})$ in logarithmic-scale are ($\bar{\gamma}$+10dB, $\bar{\gamma}$, $\bar{\gamma}$), ($\bar{\gamma}$, $\bar{\gamma}$+10dB, $\bar{\gamma}$) and ($\bar{\gamma}$, $\bar{\gamma}$, $\bar{\gamma}$), respectively. In each case, the average BEP with LAR-$\alpha$ cooperation is simulated and full diversity is verified for $\bar{\gamma}$ large enough. When $\bar{\gamma}_{sr}$ or $\bar{\gamma}_{rd}$ is 10dB higher than others, performance improves by approximately 2dB relative to the symmetric scenario. Fig. 5 corroborates that LAR-$\alpha$ works well wherever $R$ is located. For this reason, we fix the channel setting to $(\bar{\gamma}_{sr}, \bar{\gamma}_{rd}, \bar{\gamma}_{sd})$=$(\bar{\gamma}, \bar{\gamma}, \bar{\gamma})$ in the ensuing tests; and for a fair comparison among different schemes, we draw the average BEP curves with respect to $\bar{\gamma}_{tot} = \bar{\gamma}(1 + E[\alpha])$, where $E[\alpha]$ is the average power scaling at the relay.

We also compare with two AF schemes in [13] which rely on optimizing power allocation. Fig. 5 shows that LAR-$\alpha$ outperforms the SNR-optimum scheme in [13] (which performs slightly worse than the outage-optimum scheme in [13]) because it loses diversity. Recall that although AF does not need feedback from $D$, it requires instantaneous CSI of the $S \rightarrow R$ link at $D$, which is harder to acquire in practice than LAR-$\alpha$. Fig. 5 also depicts the DF of [14], where power allocation is optimized too, but $D$ must have instantaneous CSI of all links ($S \rightarrow R$, $R \rightarrow D$, $S \rightarrow D$). At any time instant, only the signal with highest instantaneous SNR is demodulated at $D$, where the SNR of the relay link is defined as the minimum SNR of the $S \rightarrow R$ and $R \rightarrow D$ links. In the simulation, we set the threshold SNR=0dB and numerically determined the power allocation coefficients for $S$ and $R$. As verified by Fig. 5, this type of selection achieves full diversity but is somewhat inferior with respect to coding gain when compared to LAR-$\alpha$.

**Test Case 2 (different scaling factors):** Average BEP performance of LAR with various scaling factors is depicted in Fig. 6. With $\bar{\gamma}_{rd}$ known at $R$, LAR-$\alpha$ outperforms other schemes and achieves full diversity order, which corroborates the analysis in Subsection IV-B. For LAR$-\alpha(\beta)$, we test two cases, namely $\beta = 1/2$ and $\beta = 2$, corresponding to approximately 3dB underestimation and overestimation of $\alpha$,

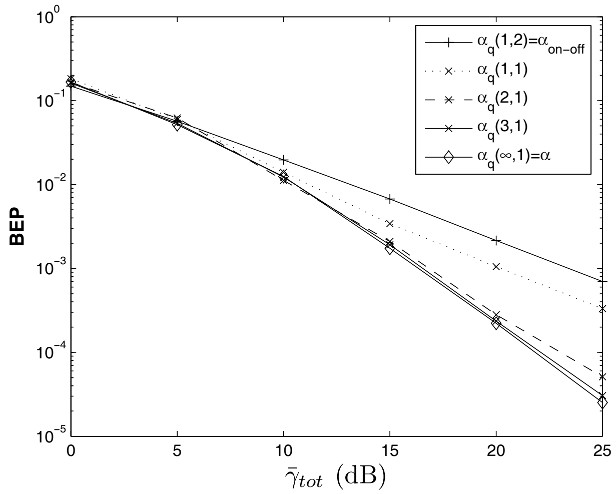


Fig. 7. BEP comparison for LAR-$\alpha_q$.

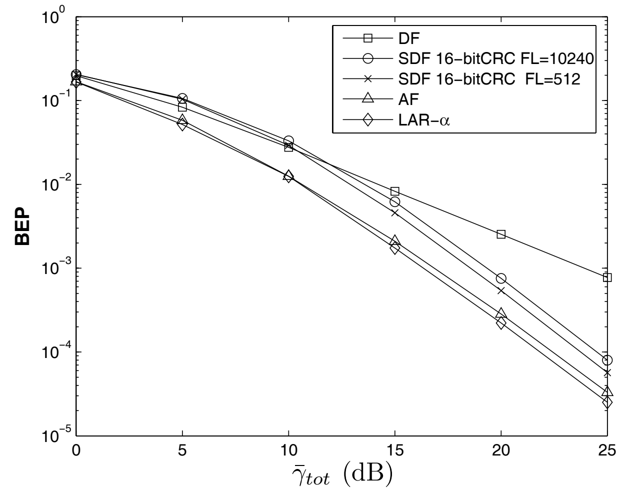


Fig. 8. BEP comparison for various relay strategies.

respectively. Both incur only 1dB loss in average BEP, which confirms the robustness of LAR-$\alpha$ to feedback errors. LAR-$\alpha'$ and LAR-$\alpha''$ incur degradation in error performance relative to LAR-$\alpha$, but outperform the non-cooperative single-input single-output (SISO) system, which only achieves diversity order one. In addition to the required feedback, the overhead here compared to SISO may include preambles for packet detection at the relay and synchronization at the destination. As expected, with instantaneous $\gamma_{rd}$ known at $R$, the LAR-$\alpha_{inst}$ as in (5) benchmarks the performance of all other schemes.

**Test Case 3 (quantization effects):** Fig. 7 illustrates average BEP performance of relay transmissions with hard power scaling coefficient $\alpha_q$ in (9). Surprisingly, with 3-bit quantization, $\alpha_q(3,1)$ yields average BEP as good as the un-quantized $\alpha$ which corresponds to $\alpha_q(\infty,1)$. When 1 or 2 bits are used for quantization, there is error performance loss at high SNR. Diversity order 1 is attained both by $\alpha_q(1,2)=\alpha_{on-off}$ and $\alpha_q(1,1)$, with the latter exhibiting a higher coding gain.

**Test Case 4 (comparison among DF, AF and SDF):** Fig. 8 compares LAR-$\alpha$ against various popular relay strategies, namely, DF, AF and SDF. While it affords the simplest implementation in practice, DF exhibits inferior error performance due to the diversity loss. Although based on analog processing, AF does not outperform LAR-$\alpha$, because it utilizes power inefficiently at the relay. When it comes to adaptive regenerative protocols, the proposed LAR-$\alpha$ outperforms also SDF. [2] Taking into account the tradeoff between redundancy and detection error probability of the CRC code, we verify that although full diversity is achieved, SDF does not lead to as good BEP performance as LAR-$\alpha$ over the practical SNR range.

**Test Case 5 (general network topology):** Fig. 9 tests generalizations and validates the full-diversity claims of LAR-$\alpha$ for multiple branches and a single relay per branch. The relays operate in parallel over orthogonal channels, with all

[2]Following the standard codes CRC-CCITT (used in X.25) and CRC-ANSI (used in DECNET) [17], we use 16-bit CRC and frame length of 512 and 10,240.

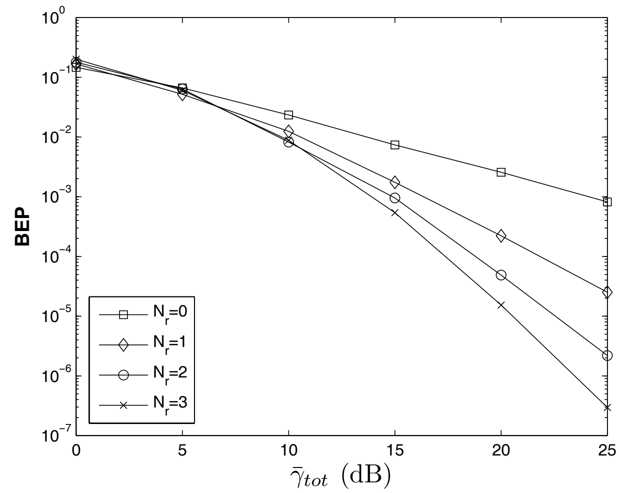


Fig. 9. BEP comparison for LAR-$\alpha$ and LAR-$\alpha_q(3,1)$ in multi-branch relay transmissions.

end-to-end links having identical average SNR $\bar{\gamma}$. Hence, in this simulation we have $\bar{\gamma}_{tot}=\bar{\gamma}(1+N_rE[\alpha])$, where $N_r$ denotes the number of relays. We note that in this scenario, the number of arriving paths to $D$ equals the number of branches, namely $N_r+1$. The case $N_r=0$ corresponds to the non-cooperative SISO setup. By inspecting the slope of the average BEP curves, we can verify that in each scheme, full diversity order of $N_r+1$ is achieved with $\alpha$ and even with $\alpha_q(3,1)$ at low-medium SNR.

Fig. 10 tests a multi-hop transmission in a two-branch system. BEP is simulated without direct link and with equal number of relays per branch. The relays are equally spaced between $S$ and $D$ with path-loss exponent equal to 3. Fig. 10 confirms that full diversity 2 is achieved regardless of the number of hops.

**Test Case 6 (higher constellations and channel coding):** To check modulations other than QPSK, we also tested BPSK and 16-QAM for LAR-$\alpha$. As shown in Fig. 11, QPSK and BPSK have identical error performance for the same average bit-

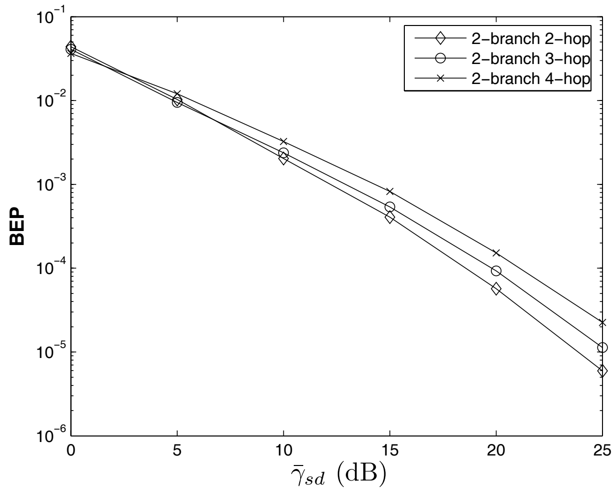


Fig. 10. BEP comparison for LAR-$\alpha$ in multi-hop relay transmissions.

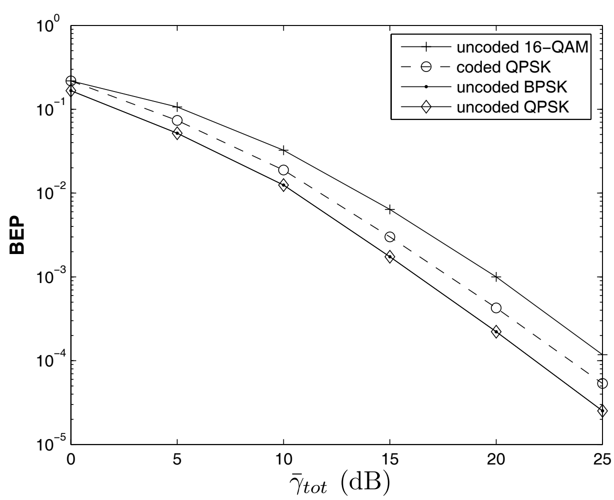


Fig. 11. BEP comparison for LAR-$\alpha$ using uncoded cooperation with BPSK, QPSK, 16-QAM, and coded cooperation with QPSK.

SNR. While attaining the full diversity gain 16-QAM incurs, as expected, loss in coding gain relative to QPSK.

As we mentioned in Subsection V-A, LAR-$\alpha$ can also improve performance of coded cooperation when one allows $R$ to decode and re-encode the received symbols but forward the parity bits instead of the information bits to the destination. Using a convolutional code with rate $1/2$ and setting the block length equal to $50$, we depict the resulting BEP curve in the same figure for comparison. Surprisingly, although coded cooperation with LAR-$\alpha$ achieves full diversity, it performs worse than uncoded LAR-$\alpha$ because of potential error propagation within the block.

**Test Case 7 (general fading channel):** Finally, we test average BEP performance of LAR-$\alpha$ in fading channels other than Rayleigh. As depicted in Fig. 12, Ricean fading achieves full diversity as Rayleigh, which is a special case of Ricean with $K = 0$; while increasing $K$ further increases the coding gain. When all channels undergo Nakagami-$m$ fading, the full diversity is $2m$, which is $4$ when $m = 2$, as verified by Fig. 12.

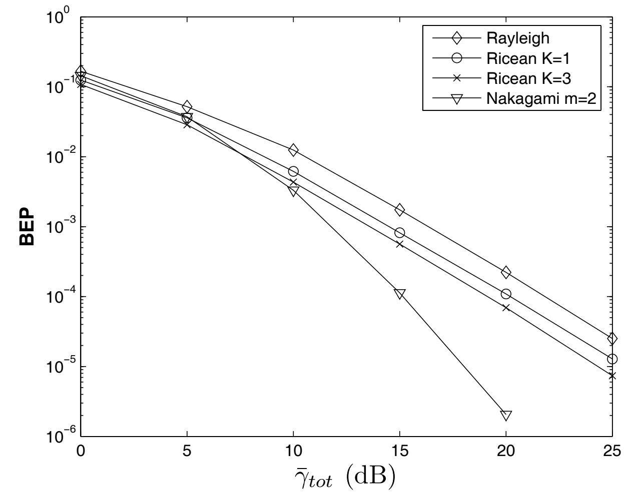


Fig. 12. BEP with LAR-$\alpha$ applied to various fading channels.

## VII. Conclusions

We developed a class of novel LAR strategies for cooperative communication systems. We proved that with a soft power scaling $\alpha$, full diversity can be achieved without using CRC codes, feeding back or forwarding any instantaneous CSI. LAR-$\alpha$ is applicable to both uncoded and coded cooperation, regardless of the underlying modulation, network size, or channel SNR settings. Compared to existing relay strategies, LAR-$\alpha$ is power efficient, full diversity achieving and readily implementable in practice. Simulations demonstrate that LAR-$\alpha$ is also robust to quantization as well as feedback errors, and outperforms existing relay strategies in terms of average BEP performance. [3]

## Appendix

### A. *Proof of Lemma 1*

Using the inequality $Q[x] \leq \frac{1}{2}\exp(-x^2/2)$, we can easily verify that

$$\begin{aligned} E[P_1^b] \leq & \int_0^\infty \frac{1}{2\bar{\gamma}_{sd}} \exp(-\gamma_{sd} - \frac{\gamma_{sd}}{\bar{\gamma}_{sd}}) d\gamma_{sd} \\ & \times \int_0^\infty \int_0^\infty \frac{1}{\bar{\gamma}_{sr}\bar{\gamma}_{rd}} \exp(-\gamma'_{rd} - \frac{\gamma_{sr}}{\bar{\gamma}_{sr}} - \frac{\gamma_{rd}}{\bar{\gamma}_{rd}}) d\gamma_{sr} d\gamma_{rd} \\ = & \frac{1}{2(1+\bar{\gamma}_{sd})} \int_0^\infty \frac{\exp(-\gamma_{sr}/\bar{\gamma}_{sr})}{(1+\alpha(\beta)\bar{\gamma}_{rd})\bar{\gamma}_{sr}} d\gamma_{sr}. \end{aligned} \quad (29)$$

Substituting the $\alpha(\beta)$ from (8) to the integral in (29), we have

$$\begin{aligned} & \int_0^\infty \frac{\exp(-\gamma_{sr}/\bar{\gamma}_{sr})}{(1+\alpha(\beta)\bar{\gamma}_{rd})\bar{\gamma}_{sr}} d\gamma_{sr} \\ = & \frac{\beta \exp(\beta/\bar{\gamma}_{sr})}{\bar{\gamma}_{sr}} \left[ \mathrm{E}_1(\frac{\beta}{\bar{\gamma}_{sr}}) - \mathrm{E}_1(\frac{\beta(1+\bar{\gamma}_{rd})}{\bar{\gamma}_{sr}}) \right] + \frac{\exp(-\beta\bar{\gamma}_{rd}/\bar{\gamma}_{sr})}{1+\bar{\gamma}_{rd}} \\ \leq & \frac{\beta}{\bar{\gamma}_{sr}} \ln(1 + \frac{\bar{\gamma}_{sr}}{\beta}) + \frac{1}{1+\bar{\gamma}_{rd}} \exp(-\frac{\beta\bar{\gamma}_{rd}}{\bar{\gamma}_{sr}}) \end{aligned} \quad (30)$$

[3]The views and conclusions contained in this document are those of the authors and should not be interpreted as representing the official policies, either expressed or implied, of the Army Research Laboratory or the U. S. Government.

where the last inequality comes from $\mathrm{E}_1(x) \geq 0$ and the following property [18, eq. (5.1.20)]: $\frac{1}{2}\ln(1+\frac{2}{x}) < \exp(x)\mathrm{E}_1(x) < \ln(1+\frac{1}{x})$, both for all $x > 0$.

Combining (29) and (30), we arrive at the desired result $E[P_1^b] \leq \tilde{P}_1^b$, where

$$\tilde{P}_1^b = \frac{1}{2(1+\bar{\gamma}_{sd})}\left[\frac{\beta}{\bar{\gamma}_{sr}}\ln(1+\frac{\bar{\gamma}_{sr}}{\beta}) + \frac{1}{1+\bar{\gamma}_{rd}}\exp(-\frac{\beta\bar{\gamma}_{rd}}{\bar{\gamma}_{sr}})\right] \quad (31)$$

and $\lim_{\bar{\gamma}\to\infty} -\log\tilde{P}_1^b/\log\bar{\gamma} = 2$.

### B. *Proof of Lemma 2*

Partitioning the integration interval and using the upper bound of the $Q[x]$ function, we find that $E[P_2^b] \leq P_A + P_B$, where

$$P_A := \int_0^\infty\int_0^\infty\int_{\gamma'_{rd}}^\infty \frac{1}{2}\exp(-\gamma_{sr})\frac{1}{2}\exp\left[-\frac{(\gamma_{sd}-\gamma'_{rd})^2}{\gamma_{sd}+\gamma'_{rd}}\right] \times p(\gamma_{sd})p(\gamma_{sr})p(\gamma_{rd})d\gamma_{sd}d\gamma_{sr}d\gamma_{rd}$$

$$P_B := \int_0^\infty\int_0^\infty\int_0^{\gamma'_{rd}} \frac{1}{2}\exp(-\gamma_{sr}) \times p(\gamma_{sd})p(\gamma_{sr})p(\gamma_{rd})d\gamma_{sd}d\gamma_{sr}d\gamma_{rd}.$$

Now we rewrite

$$P_A = \int_0^\infty\int_0^\infty \frac{1}{2}\exp(-\gamma_{sr})\frac{1}{\bar{\gamma}_{sr}}\exp(-\frac{\gamma_{sr}}{\bar{\gamma}_{sr}})\frac{1}{\bar{\gamma}_{rd}}\exp(-\frac{\gamma_{rd}}{\bar{\gamma}_{rd}}) \times f_A(\gamma'_{rd})d\gamma_{sr}d\gamma_{rd}$$

where

$$\begin{aligned} f_A(\gamma'_{rd}) &:= \int_{\gamma'_{rd}}^\infty \frac{1}{2}\exp\left[-(\gamma_{sd}+\gamma'_{rd}-\frac{4\gamma_{sd}\gamma'_{rd}}{\gamma_{sd}+\gamma'_{rd}})\right]\frac{1}{\bar{\gamma}_{sd}}\exp(-\frac{\gamma_{sd}}{\bar{\gamma}_{sd}})d\gamma_{sd} \\ &\leq \int_{\gamma'_{rd}}^\infty \frac{1}{2}\exp\left[-(\gamma_{sd}+\gamma'_{rd}-2\sqrt{\gamma_{sd}\gamma'_{rd}})\right]\frac{1}{\bar{\gamma}_{sd}}\exp(-\frac{\gamma_{sd}}{\bar{\gamma}_{sd}})d\gamma_{sd} \\ &\leq \frac{\exp(-\gamma'_{rd}/\bar{\gamma}_{sd})}{2(1+\bar{\gamma}_{sd})^2}\left[1+\bar{\gamma}_{sd}+\sqrt{1+\bar{\gamma}_{sd}}\sqrt{\pi\bar{\gamma}_{sd}\gamma'_{rd}}\right] =: \tilde{f}_A(\gamma'_{rd}). \end{aligned}$$

So $P_A \leq \tilde{P}_A := \int_0^\infty \frac{1}{2\bar{\gamma}_{sr}}\exp(-\gamma_{sr} - \frac{\gamma_{sr}}{\bar{\gamma}_{sr}})g(\gamma_{sr})d\gamma_{sr}$, where

$$g(\gamma_{sr}) = \int_0^\infty \frac{1}{\bar{\gamma}_{rd}}\exp(-\frac{\gamma_{rd}}{\bar{\gamma}_{rd}})\tilde{f}_A(\gamma'_{rd})d\gamma_{rd} =$$

$$\begin{cases} g^l := \frac{2\beta\bar{\gamma}_{sd}\sqrt{(1+\bar{\gamma}_{sd})(\gamma_{sr}+\beta\bar{\gamma}_{sd})}+\pi\beta\bar{\gamma}_{sd}^2\sqrt{\gamma_{sr}}}{4(1+\bar{\gamma}_{sd})^{3/2}(\gamma_{sr}+\beta\bar{\gamma}_{sd})^{3/2}}, & \text{if } \gamma_{sr} \leq \beta\bar{\gamma}_{rd}, \\ g^h := \frac{2\bar{\gamma}_{sd}\sqrt{(1+\bar{\gamma}_{sd})(\bar{\gamma}_{rd}+\bar{\gamma}_{sd})}+\pi\bar{\gamma}_{sd}^2\sqrt{\gamma_{rd}}}{4(1+\bar{\gamma}_{sd})^{3/2}(\bar{\gamma}_{rd}+\bar{\gamma}_{sd})^{3/2}}, & \text{if } \gamma_{sr} \geq \beta\bar{\gamma}_{rd}. \end{cases}$$

Subsequently, we partition the integral defining $\tilde{P}_A$ to write $\tilde{P}_A = \tilde{P}_A^l + \tilde{P}_A^h$, where

$$\begin{aligned} \tilde{P}_A^l &:= \int_0^{\beta\bar{\gamma}_{rd}} \frac{1}{2\bar{\gamma}_{sr}}\exp(-\gamma_{sr} - \frac{\gamma_{sr}}{\bar{\gamma}_{sr}})g^l d\gamma_{sr} \\ &\leq \frac{1}{4\bar{\gamma}_{sr}\bar{\gamma}_{sd}} + \frac{\pi^{3/2}\sqrt{\bar{\gamma}_{sr}\bar{\gamma}_{sd}}}{16\sqrt{\beta}(\bar{\gamma}_{sr})^{3/2}(\bar{\gamma}_{sd})^{3/2}}, \quad (32) \\ \tilde{P}_A^h &:= \int_{\beta\bar{\gamma}_{rd}}^\infty \frac{1}{2\bar{\gamma}_{sr}}\exp(-\gamma_{sr} - \frac{\gamma_{sr}}{\bar{\gamma}_{sr}})g^h d\gamma_{sr} \\ &= \exp\left[-\frac{\beta\bar{\gamma}_{rd}(1+\bar{\gamma}_{sr})}{\bar{\gamma}_{sr}}\right]\frac{g^h}{2(1+\bar{\gamma}_{sr})}. \quad (33) \end{aligned}$$

As far as $P_B$ is concerned, we first integrate with respect to $\gamma_{sd}$ and $\gamma_{rd}$ to arrive at

$$P_B = \int_0^\infty \frac{1}{2\bar{\gamma}_{sr}}\exp(-\gamma_{sr} - \frac{\gamma_{sr}}{\bar{\gamma}_{sr}})\frac{\min(\gamma_{sr},\beta\bar{\gamma}_{rd})}{\min(\gamma_{sr},\beta\bar{\gamma}_{rd})+\beta\bar{\gamma}_{sd}}d\gamma_{sr}.$$

Again, partitioning the integration interval, we obtain $P_B = P_B^l + P_B^h$, where

$$\begin{aligned} P_B^l &:= \int_0^{\beta\bar{\gamma}_{rd}} \frac{1}{2\bar{\gamma}_{sr}}\exp(-\gamma_{sr} - \frac{\gamma_{sr}}{\bar{\gamma}_{sr}})\frac{\gamma_{sr}}{\beta\bar{\gamma}_{sd}+\gamma_{sr}}d\gamma_{sr} \\ &\leq \frac{1}{2\left[\bar{\gamma}_{sr}+\beta\bar{\gamma}_{sd}(1+\bar{\gamma}_{sr})\right]} \quad (34) \\ P_B^h &:= \int_{\beta\bar{\gamma}_{rd}}^\infty \frac{1}{2\bar{\gamma}_{sr}}\exp(-\gamma_{sr} - \frac{\gamma_{sr}}{\bar{\gamma}_{sr}})\frac{\bar{\gamma}_{rd}}{\bar{\gamma}_{rd}+\bar{\gamma}_{sd}}d\gamma_{sr} \\ &\leq \frac{1}{2}\exp\left[-\frac{\beta\bar{\gamma}_{rd}(1+\bar{\gamma}_{sr})}{\bar{\gamma}_{sr}}\right]. \quad (35) \end{aligned}$$

Notice that $E[P_2^b]$ can be upper bounded by the sum of the right-hand-side (RHS) of (32), (33), (34), and (35). Because each of the four terms decays with exponent at least two, we deduce readily that their sum, denoted as $\tilde{P}_2^b$, can be approximated by $\tilde{P}_2^b \approx (\kappa_2\bar{\gamma})^{-2}$ as $\bar{\gamma} \to \infty$, where $\kappa_2$ is a constant which depends on $\sigma_{sr}^2, \sigma_{sd}^2, \sigma_{rd}^2$ and $\beta$; hence, $\lim_{\bar{\gamma}\to\infty} -\log\tilde{P}_2^b/\log\bar{\gamma} = 2$.

### C. *Proof of Proposition 2*

First we will prove that full diversity cannot be reached with two-level power scaling ($N_q = 1$) and any $\beta > 0$. We consider BPSK but as before the claims carry over to higher constellations too. Since $P^b$ in (17) is the sum of two positive terms, to show that full diversity cannot be achieved, it suffices to show that the first term, denoted as $P_f^b$, does not decay with exponent two when power is scaled with $\alpha_q(1,\beta)$. We first rely on the bound of the $Q[x]$ function to obtain

$$P_f^b \geq \left[1 - \frac{1}{2}\exp(-\gamma_{sr})\right]\left\{\frac{\exp[-(\gamma_{sd}+\gamma'_{rd})]}{2\sqrt{\pi}\sqrt{\gamma_{sd}+\gamma'_{rd}+2}}\right\}. \quad (36)$$

Upon defining $\Phi(\gamma_{sr}) := \frac{2\exp(\gamma_{sr})-1}{2\bar{\gamma}_{rd}\bar{\gamma}_{sr}\sqrt{\pi}}\exp\left[-\frac{\gamma_{sr}(1+\bar{\gamma}_{sr})}{\bar{\gamma}_{sr}}\right]$, we can further lower bound $E[P_f^b]$ as

$$\begin{aligned} E[P_f^b] &\geq \int_0^\infty\int_0^\infty \frac{\exp\left[-\gamma_{rd}(\alpha_q(1,\beta)+1/\bar{\gamma}_{rd})\right]}{(2+3\bar{\gamma}_{sd})\sqrt{2+\alpha_q(1,\beta)\gamma_{rd}}}\Phi(\gamma_{sr})d\gamma_{sr}d\gamma_{rd} \\ &= \int_0^\infty \frac{\pi\exp[2+2/(\alpha_q(1,\beta)\bar{\gamma}_{rd})]}{(2+3\bar{\gamma}_{sd})\alpha_q(1,\beta)\sqrt{\pi+\pi/(\alpha_q(1,\beta)\bar{\gamma}_{rd})}} \\ &\quad \times \mathrm{Erfc}\left[\sqrt{2+2/(\alpha_q(1,\beta)\bar{\gamma}_{rd})}\right]\Phi(\gamma_{sr})d\gamma_{sr} \\ &\geq P_C + P_D \end{aligned}$$

where we made use of the lower bound of $\mathrm{Erfc}[x]$ [19], substituted $\alpha_q(1,\beta)$ from (9) and defined

$$P_C := \int_0^{\beta\bar{\gamma}_{rd}} \frac{\bar{\gamma}_{rd}}{\sqrt{2}(2+3\bar{\gamma}_{sd})}\Phi(\gamma_{sr})d\gamma_{sr}$$

$$P_D := \int_{\beta\bar{\gamma}_{rd}}^\infty \frac{\bar{\gamma}_{rd}}{\sqrt{(2+4\bar{\gamma}_{rd})(1+\bar{\gamma}_{rd})}(2+3\bar{\gamma}_{sd})}\Phi(\gamma_{sr})d\gamma_{sr}.$$

Since both integrals are positive, $P_C$ and $P_D$ are also positive. And for this reason, it suffices to show that one of them cannot achieve full diversity. After integration, we have

$$P_C = \frac{1}{2\sqrt{2\pi}(2+3\bar{\gamma}_{sd})}\left\{2\left[1-\exp\left(-\frac{\beta\bar{\gamma}_{rd}}{\bar{\gamma}_{sr}}\right)\right] - \frac{1}{1+\bar{\gamma}_{sr}}\left[1-\exp\left(-\frac{\beta\bar{\gamma}_{rd}(1+\bar{\gamma}_{sr})}{\bar{\gamma}_{sr}}\right)\right]\right\}.$$

Since $(\bar{\gamma}_{sr}, \bar{\gamma}_{sd}, \bar{\gamma}_{rd}) = (\sigma_{sr}^2\bar{\gamma}, \sigma_{sd}^2\bar{\gamma}, \sigma_{rd}^2\bar{\gamma})$, $P_C$ decays as $(\kappa_3\bar{\gamma})^{-1}$ when $\bar{\gamma} \to \infty$, with $\kappa_3$ a constant depending on $\sigma_{sr}^2, \sigma_{sd}^2, \sigma_{rd}^2$ and $\beta$. So full diversity two cannot be achieved here using $\alpha_q(1,\beta)$.

To prove that the diversity order with LAR-$\alpha_q(1,\beta)$ is 1, we will show that $E[P^b] \le \tilde{P}^b \overset{\bar{\gamma}\to\infty}{\approx} (\kappa_4\bar{\gamma})^{-1}$, for some constant $\kappa_4$. Checking (17) again, we can write

$$\begin{aligned} P^b &\le Q\left[\sqrt{2(\gamma_{sd}+\gamma'_{rd})}\right] + Q\left[\sqrt{2\gamma_{sr}}\right] \\ &\le \frac{1}{2}\exp\left[-(\gamma_{sd}+\alpha_q(1,\beta)\gamma_{rd})\right] + \frac{1}{2}\exp\left[-\gamma_{sr}\right]. \quad (37) \end{aligned}$$

After substituting $\alpha_q(1,\beta)$ and taking expectation on both sides of (37), one can easily obtain

$$E[P^b] \le \tilde{P}^b = \frac{1+\bar{\gamma}_{rd}[1-\exp(-\beta\bar{\gamma}_{rd}/\bar{\gamma}_{sr})]}{2(1+\bar{\gamma}_{rd}+\bar{\gamma}_{sd}+\bar{\gamma}_{rd}\bar{\gamma}_{sd})} + \frac{1}{2(1+\bar{\gamma}_{sr})}.$$

It follows that $\tilde{P}^b \overset{\bar{\gamma}\to\infty}{\approx} (\kappa_4\bar{\gamma})^{-1}$, with $\kappa_4$ some constant depending on $\sigma_{sr}^2, \sigma_{sd}^2, \sigma_{rd}^2$ and $\beta$. Hence, we have proved that the diversity order achieved with $\alpha_q(1,\beta)$ is exactly 1.

To extend the loss of diversity where scalings have more than two levels ($N_q > 1$), it suffices to note that values of $(\gamma_{sr}, \bar{\gamma}_{rd})$ for which $\alpha_q(N_q,\beta) = 0$ or $1$ will lead to diversity loss as we proved for the $N_q = 1$ case.

## REFERENCES


[1] A. Sendonaris, E. Erkip, and B. Aazhang, "User cooperation diversity–part I: system description," *IEEE Trans. Commun.*, vol. 51, no. 11, pp. 1927–1938, Nov. 2003.

[2] ——, "User cooperation diversity–part II: implementation aspects and performance analysis," *IEEE Trans. Commun.*, vol. 51, no. 11, pp. 1939–1948, Nov. 2003.

[3] J. N. Laneman, D. N. C. Tse, and G. W. Wornell, "Cooperative diversity in wireless networks: efficient protocols and outage behavior," *IEEE Trans. Inform. Theory*, vol. 50, no. 12, pp. 3062–3080, Dec. 2004.

[4] A. Ribeiro, X. Cai, and G. B. Giannakis, "Symbol error probabilities for general cooperative links," *IEEE Trans. Wireless Commun.*, vol. 4, no. 3, pp. 1264–1273, May 2005.

[5] E. Zimmermann, P. Herhold, and G. Fettweis, "On the performance of cooperative diversity protocols in practical wireless systems," in *Proc. 58th Vehicular Technology Conference*, vol. 4, Orlando, FL, Oct. 6-9 2003, pp. 2212–2216.

[6] T. Wang, A. Cano, G. Giannakis, and J. Laneman, "High-performance cooperative demodulation with decode-and-forward relays," *IEEE Trans. Commun.*, vol. 55, no. 7, pp. 1427–1438, July 2007.

[7] M. Janani, A. Hedayat, T. Hunter, and A. Nosratinia, "Coded cooperation in wireless communications: space-time transmission and iterative decoding," *IEEE Trans. Signal Processing*, vol. 52, no. 2, pp. 362–371, Feb. 2004.

[8] P. Tarasak, H. Minn, and V. Bhargava, "Differential modulation for two-user cooperative diversity systems," *IEEE J. Select. Areas Commun.*, vol. 23, no. 9, pp. 1891–1900, Sept. 2005.

[9] T. M. Cover and A. E. Gamal, "Capacity theorems for the relay channel," *IEEE Trans. Inform. Theory*, vol. 25, no. 5, pp. 572–584, Sept. 1979.

[10] G. Kramer, M. Gastpar, and P. Gupta, "Cooperative strategies and capacity theorems for relay networks," *IEEE Trans. Inform. Theory*, vol. 51, no. 9, pp. 3037–3063, Sept. 2005.

[11] E. W. Weisstein, "En-Function," *From MathWorld–A Wolfram Web Resource*, http://mathworld.wolfram.com/En-Function.html.

[12] P. A. Anghel, G. Leus, and M. Kaveh, "Distributed space-time cooperative systems with regenerative relays," *IEEE Trans. Wireless Commun.*, vol. 5, no. 11, pp. 3130–3141, Nov. 2006.

[13] X. Deng and A. M. Haimovich, "Power allocation for cooperative relaying in wireless networks," *IEEE Commun. Lett.*, vol. 9, no. 11, pp. 994–996, Nov. 2005.

[14] M. O. Hasna and M. S. Alouini, "Optimal power allocation for relayed transmissions over rayleigh-fading channels," *IEEE Trans. Wireless Commun.*, vol. 3, no. 6, pp. 1999–2004, Nov. 2004.

[15] J. G. Proakis, *Digital Communications*, 4th ed. McGraw-Hill Higher Education, 2001.

[16] J. Adeane, M. R. D. Rodrigues, and I. J. Wassell, "Characterisation of the performance of cooperative networks in Ricean fading channels," in *Proc. 12th International Conference on Telecommunications*, Cape Town, South Africa, May 3-6, 2005.

[17] G. Castagnoli, J. Ganz, and P. Graber, "Optimum cyclic redundancy check codes with 16-bit redundancy," *IEEE Trans. Commun.*, vol. 38, no. 1, pp. 111–114, 1990.

[18] M. Abramowitz and I. A. Stegun, *Handbook of Mathematical Functions with Formulas, Graphs, and Mathematical Tables*. U.S. Department of Commerce, 1972.

[19] E. W. Weisstein, "Erfc." *From MathWorld–A Wolfram Web Resource*, http://mathworld.wolfram.com/Erfc.html.


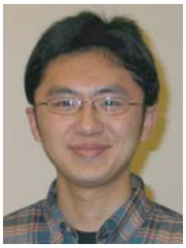


**Tairan Wang** (S'05) received his B.S. degree in Electrical Engineering and Information Science in 2003, from the University of Science and Technology of China (USTC). He is currently a Ph.D. candidate in the Department of Electrical and Computer Engineering at the University of Minnesota (UMN). His research interests lie in the areas of communication theory, information theory and networking. Current research focuses on wireless cooperative communications, game theory, network coding, and wireless sensor networks.



**Georgios B. Giannakis** (F'97) received his Diploma in Electrical Engr. from the Ntl. Tech. Univ. of Athens, Greece, 1981. From 1982 to 1986 he was with the Univ. of Southern California (USC), where he received his MSc. in Electrical Engineering, 1983, MSc. in Mathematics, 1986, and Ph.D. in Electrical Engr., 1986. Since 1999 he has been a professor with the Univ. of Minnesota, where he now holds an ADC Chair in Wireless Telecommunications in the ECE Department and serves as director of the Digital Technology Center.

His general interests span the areas of communications, networking and statistical signal processing, subjects on which he has published more than 275 journal papers, 450 conference papers, two edited books and two research monographs. Current research focuses on complex-field and network coding, cooperative wireless communications, cognitive radios, cross-layer designs, mobile ad hoc networks and wireless sensor networks. He is the (co-) recipient of six paper awards from the IEEE Signal Processing (SP) and Communications Societies including the G. Marconi Prize Paper Award in Wireless Communications. He also received Technical Achievement Awards from the SP Society (2000), from EURASIP (2005), a Young Faculty Teaching Award and the G. W. Taylor Award for Distinguished Research from the University of Minnesota. He is a Fellow of EURASIP, has served the IEEE in a number of posts, and is currently a Distinguished Lecturer for the IEEE-SP Society.



**Renqiu Wang** (M'07) received her B.S. degree in Electrical Engineering and Information Science from the University of Science and Technology of China (USTC), 1998, the M.Sc. degree in Electrical and Computer Engineering from the University of Minnesota, 2003, and Ph.D. in Electrical and Computer Engineering from the University of Minnesota, 2006. She is now with the Qualcomm Inc. Her interests are in the general areas of signal processing, communications, and information theory and more focus on MIMO communications, coding, and cooperative communications.